

Effect of Overaging on Fatigue Crack Propagation of 2024 T3 Aluminum Alloy

A.T. Tzamtzis^{1,*}, A.T. Kermanidis²

Laboratory of Mechanics and Strength of Materials, Department of Mechanical Engineering,
University of Thessaly, Volos, Greece

¹atzam@uth.gr

²akermanidis@mie.uth.gr.

ABSTRACT

The effect of controlled overaging on fatigue crack propagation (Stage II) in 2024-T3 aluminum alloy was experimentally investigated. Overaging was performed by subjecting the material from initial T3 state to appropriate aging conditions. Fatigue crack growth experiments were conducted to assess the influence of artificial aging on fatigue crack growth resistance. The experimental results showed that overaging enhances the fatigue crack propagation behavior at intermediate ΔK values compared to the T3 state and fatigue crack growth resistance was found to increase with the magnitude of overaging temperature. The reduction of fatigue crack growth rate in the overaged alloy compared to T3 material was associated with crack closure phenomena caused by cyclic plasticity and modification of strain hardening characteristics at the crack path.

Keywords: *aluminium alloy; fatigue crack propagation; yield strength; cyclic strain hardening; crack closure;*

1 Introduction

Heat treatable aluminum alloys offer apart from high specific properties, good fatigue crack growth resistance. Mechanical properties such as yield strength and ductility can be manipulated with the use of artificial aging [1]. In aluminum alloys overaging is associated with a material strength reduction but also a reduction of ductility [1], and therefore usually not preferable in design with specific strength considerations. On the other hand a controlled strength reduction may improve fatigue crack growth as shown in [2-4].

The effect of overaging on fatigue crack propagation of aluminum alloys near the ΔK threshold region, has been extensively investigated [e.g 5-7]. In the case of long cracks (intermediate ΔK values), limited experimental data exist which examine the influence of overaging close to peak aging on fatigue crack growth performance [5-9]. Fatigue crack growth resistance of 2024 aluminum alloy in underaged, overaged and T3 state has been shown to exhibit small differences with regard to crack propagation rates near peak aged conditions [5-6]. Garrett and Knott [8] examined the crystallographic nature of fatigue crack growth in plate, pure Al-Cu alloys and showed that fatigue life in overaged conditions was slightly shorter compared to peak-aged material. In 7xxx alloys, Desmukh et al. [9] showed that overaged 7010 aluminum alloy exhibited increased fatigue crack growth rates compared to the same material in peak aged conditions.

In the present work the effect of controlled overaging on long fatigue crack propagation of aluminum alloy 2024-T3 was investigated. Overaging was performed on the initial T3 state with specific heat treatment conditions. Subsequently, the influence of overaging on fatigue crack growth was evaluated by means of crack propagation tests under cyclic loads. The behavior was analyzed and compared with the behavior in initial T3 state.

*Corresponding author

2 Material

Sheet, 2024 aluminum alloy with thickness of 3.2 was used in T3 condition, which includes solution heat treatment at 495°C, control stretching and natural aging. The nominal chemical composition of the alloy is in (%) weight Al-4.3Cu-1.5Mg-0.6Mn. The material was tested in the longitudinal (L) direction.

3 Heat Treatment & Microstructure

The overaging temperatures were selected using the overaging curves as determined in [10]. The heat treatment temperatures were 200°C, 250°C and 300°C. The aging time selected was 15 hours. The materials produced using the above aging parameters, are referred to as A200, A250 and A300 materials respectively. Hardness measurements showed that at 200°C for 15 hours no effect on hardness was observed, while at 250°C and 300°C a decrease in hardness of 25% and 50% respectively, was achieved with regard to T3 state.

The microstructure of the material in the as received T3 condition and after artificial aging is shown in Fig.1. The T3 microstructure (Fig.1a) consists of three types of inclusions: (i) Al-Cu containing particles (ii) Al-Cu-Fe-Mn containing particles, and (iii) Al-Cu-Fe-Si-Mn containing particles, as obtained from the performed SEM/EDS analysis. The 2024-T3 microstructure is characterized by two major second-phase particles: Al_2Cu (θ' phase) and Al_2CuMg (S phase) [11].

In Fig.1b the microstructure of the alloy A200 is presented. With regard to the T3 material, inclusions seem to be unaffected, while coarsening of the metastable phases inside the grains can be observed.

In Figs.1c and 1d the microstructure of the alloys A250 and A300 are displayed. Metastable phases have dissolved from the grain boundaries, and precipitated within the grains. Precipitate-free zones (PFZs) are also evident at the grain boundaries. Coarsening of the metastable phases is more evident than in A200 material with the effect being more pronounced in material A300. Inclusions seem to be unaffected.

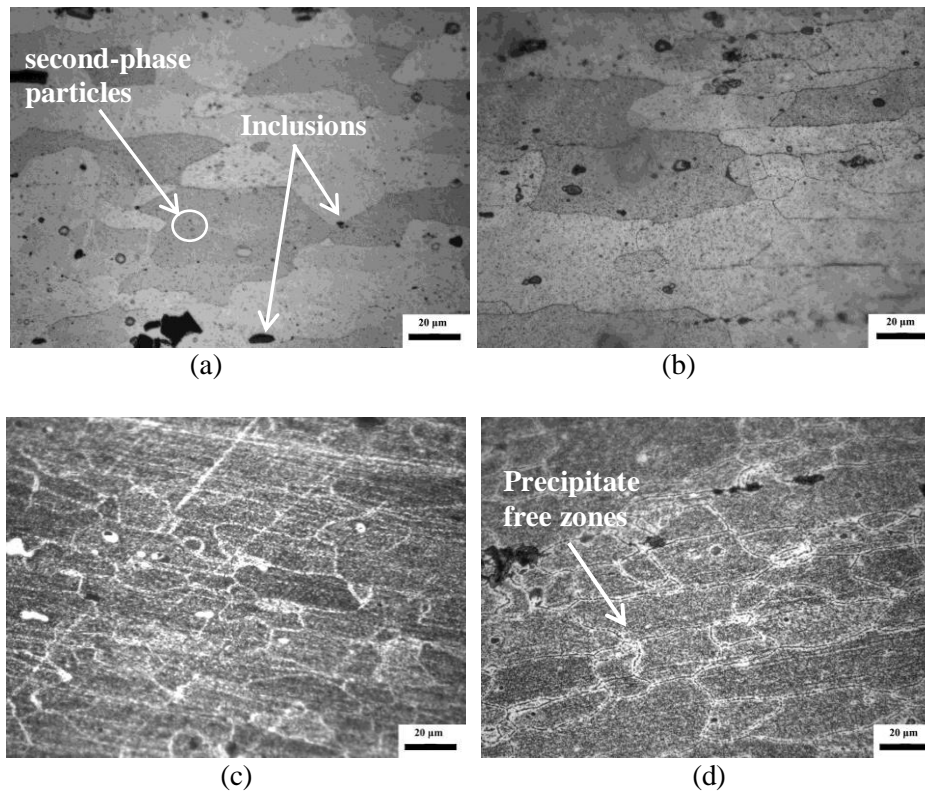


Figure 1: Microstructure of materials subjected to artificial aging (a) T3 condition (b) A200 condition (c) A250 condition (d) A300 condition

4 Testing - Discussion

4.1 Tensile behavior

Tensile tests were performed (ASTM E8M-01) to obtain the mechanical properties of the material in T3 condition and after aging treatment. The tests were carried out on subsize specimens in the L material direction. The tensile properties of the materials examined are given in Table 1, while the tensile stress-strain curves for the different aging conditions are shown in Fig.1. A gradual decrease in yield strength with aging temperature in A300 material is observed, that reaches a maximum reduction of 40% of the initial value (T3). The elongation at fracture is reduced to 60% of the initial value. A slight increase of yield strength, combined with a reduction in elongation, which is consistent with the one observed at higher aging temperatures in A200 material is observed. Increased strain hardening values were obtained with increasing overaging temperature as shown in Fig.2. The values of the strain hardening exponent n and strength coefficient H were assessed according to Eq.1 [12] and are given in Table 1. The results reveal an increase of the hardening exponent value with aging temperature, reaching an 185% increase in A300 compared to T3 material.

$$\sigma = H\varepsilon_p^n \quad (1)$$

Table 1: Tensile test results (average values)

	Yield Strength $R_{0.2}$ (MPa)	Elongation at fracture A_{25} (%)	Tensile Strength R_m (MPa)	Strain hardening exponent n	Strength coefficient H (MPa)
T3	375	15	490	0,100	380
A200	395	9.5	460	0,079	399
A250	240	10	355	0,185	265
A300	135	11	285	0,285	175

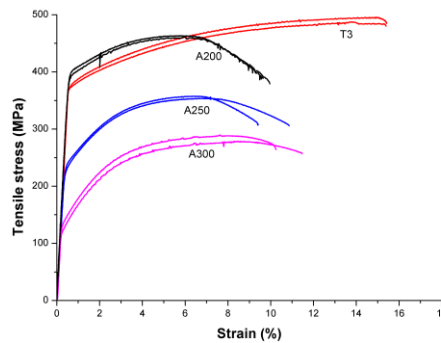


Figure 2: Tensile Stress-Strain curves of T3, A200, A250, A300 materials

4.2 Fatigue crack growth (FCG)

Fatigue crack propagation tests were carried out on compact tension C(T) specimens with a width of 60 mm in accordance with ASTM E647-00. The notch was machined parallel to the rolling direction with a constant stress ratio of $R=0.1$. The maximum stress was $\sigma_{max}= 10\text{MPa}$ and the frequency 5Hz. Crack length measurements were made using a crack opening displacement (COD) gauge. Crack growth rates were measured at an intermediate ΔK region ranging from 11 to 25 $\text{MPa}\sqrt{m}$. In total 6 FCG tests were carried out for each material to account for possible scatter effects. Crack closure measurements were performed in order to determine the minimum force at which the crack is open during cyclic loading.

In Figs. 3 and 4 the FCG results of T3, A200, A250 and A300 materials are presented. A pronounced effect of aging treatment on FCG behavior is observed in Fig 3a. Specifically, crack growth resistance is enhanced after aging treatment compared to T3 material. The FCG performance

increases with the magnitude of overaging temperature. In the case of A200 material, fatigue behavior seems unaffected by the overaging process. Fatigue lives were assessed considering also the experimental scatter in fatigue life measurements in Fig.3b. In the Figure, the experimental fatigue lives are displayed in terms of mean fatigue lives (average values of 6 tests) versus standard deviation. Fatigue crack growth rates of T3 and A200, A250 and A300 materials are compared in Fig. 4. Crack growth rates of A250 and A300 were lower than T3 material in the whole ΔK range examined, with A300 exhibiting superior crack growth resistance. The effect is more noticeable at low ΔK values. Crack growth rates in A200 material were comparable to the rates in T3 material.

In Table 2 the Paris crack growth constants C, n as determined from $da/dN-\Delta K$ curves are presented. The C value decreases with increasing aging temperature, which is consistent with the lower crack growth rates observed in overaged material.

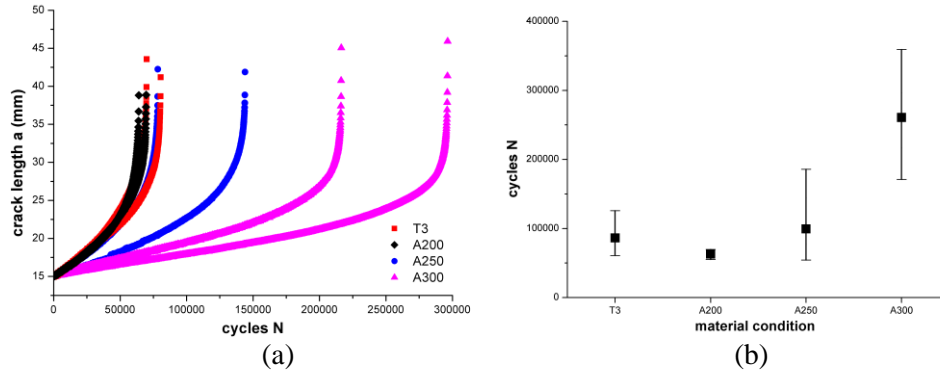


Figure 3: (a) Crack growth curves in T3 and overaged material (b) mean fatigue life results versus standard deviation in T3 and overaged conditions

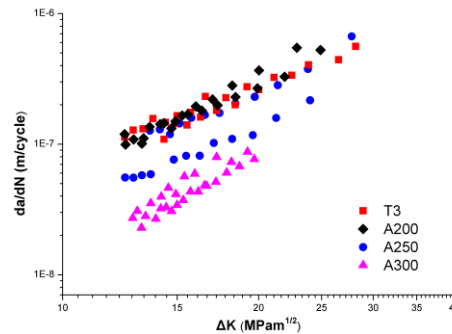


Figure 4: Fatigue crack growth rates ($da/dN-\Delta K$) in T3 and overaged material

Table 2: Paris constants calculated for the material under investigation

	Specimen	Range ΔK that used for the calculations	Paris exponent n	Paris Constant C
T3	#1	14-26	2,19	$3,5 \times 10^{-10}$
	#2	14-28	1,93	$8,88 \times 10^{-10}$
A200	#1	14-24	2,23	$3,53 \times 10^{-10}$
	#2	14-22	2,94	$5,33 \times 10^{-11}$
A250	#1	14-24	2,34	$2,29 \times 10^{-10}$
	#2	14-24	1,88	$4,88 \times 10^{-10}$
A300	#1	14-19	2,51	$5,24 \times 10^{-11}$
	#2	14-19	2,85	$1,57 \times 10^{-11}$

Measurements of crack closure during fatigue testing are presented in Fig.5a in terms of crack opening load (P_{op}/P_{max}) vs. the applied stress intensity range ΔK . As shown in the Figure, crack closure increases with increasing overaging temperature in the ΔK range examined ($11-15 \text{ MPa}\sqrt{m}$). Hence

A300 material exhibits the highest crack closure values during the test. The increase of crack closure is in agreement with the lower values of C described in the previous paragraph. In the case of A200 material, crack closure levels are slightly lower compared to T3 material in the same ΔK range. This may be associated to the slightly lower yield strength value of T3 (Fig. 2). The transition to higher crack closure values in A200 material compared to T3 at ΔK values higher than $15 \text{ MPa}\sqrt{m}$ is not intuitively understandable and requires further investigation. By taking into account the higher closure levels of T3 material in the range $11\text{-}15 \text{ MPa}\sqrt{m}$, the negligible differences in crack growth rates in the two materials can be explained.

The FCG rates for all materials in terms of effective stress intensity factor range ($da/dN\text{-}\Delta K_{\text{eff}}$) are displayed in Fig. 5b. For the calculation of the effective stress intensity range ($\Delta K_{\text{eff}} = K_{\text{max}} - K_{\text{op}}$) a mean level of P_{op} in the range $11\text{-}21 \text{ MPa}\sqrt{m}$ was used. With consideration of ΔK_{eff} values, crack growth rate levels are converging in a narrow band, which demonstrates the influence of crack closure on FCG rates.

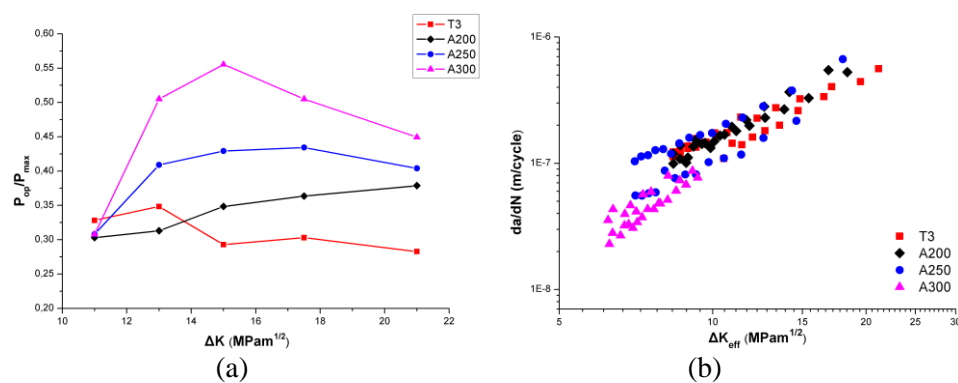


Figure 5: a) Variation of crack closure as a function of applied stress intensity range, in T3 and overaged materials b) FCG rates ($da/dN\text{-}\Delta K_{\text{eff}}$) in T3 and overaged materials

Crack closure levels determined experimentally, increase with the magnitude of aging temperature, which explains the FCG performance observed in Figs 3 and 4. Considering the possible influences on crack closure, the effects of particles, roughness surface and plasticity on the crack path [13] should be examined. Second phase particles are not expected to influence the material's performance, since the effect is more obvious in low ΔK fatigue crack growth [13]. The same applies for inclusions, which seem to be unaffected by the aging treatment (Section 3). The increased crack closure of the overaged material can be attributed to cyclic plasticity effects due to the reduction of yield strength level as well as the modification of strain hardening characteristics in the overaged state. Yield strength level reduction has been shown to favor FCG resistance due to crack tip cyclic plasticity [2-4]. This effect can lead to reduction of FCG rate via the mechanism of crack closure due to remaining plastic deformation at the crack path [14]. With increasing aging temperature, coarsening of second-phase particles with non shearable characteristics influence the hardening behavior of the material due to the Orowan bypassing mechanism of semi- or incoherent particles. For a better understanding of the influence of strain hardening on FCG, strain controlled fatigue tests to assess the cyclic strain hardening after overaging are required. This is at present an ongoing investigation.

4.3 Fractography

Fractographic analysis was performed to evaluate specific fracture characteristics during fatigue crack propagation. In the micrographs of Figs.6a and 6b taken with optical stereoscope, segments of fracture surfaces for T3 and A300 materials are presented. The fracture surface segments of A300 material are more brittle compared to T3, and are characterized by radiating ridges from the notch tip, sign of the crack changing slip planes during crack growth [15]. Thus, the fracture path includes more surface irregularities than T3, which however are expected to have small contribution to the measured

crack levels in the high ΔK region. This effect has been shown to be significant in long crack growth regime in microstructures with variations in grain morphology [16,17].

In the micrographs of Figs. 7a and 7b fracture surfaces of T3 and A300 materials taken with SEM are displayed. The micrographs show a semi-cleavage fracture pattern in T3 alloy consisting of dimples as well as cleavage facets (Fig. 7a). Fracture surfaces of A300 material included larger brittle regions compared to T3 (Fig 7b). The fracture characteristics observed in the overaged alloy agree with fracture toughness measurements performed by the authors of the present paper [18]. Despite the more brittle behavior of the overaged alloy, FCG rates are lower than those obtained in T3 material (paragraph 4.2). This inconsistency can be explained on the basis of increased levels of crack closure, in the overaged alloy.

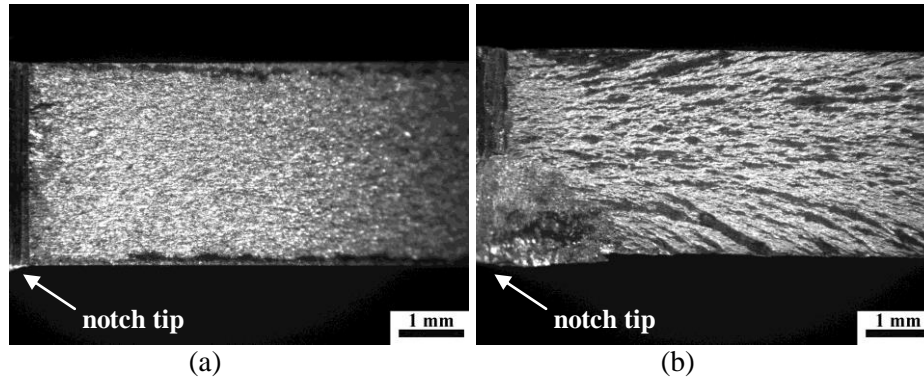


Figure 6. Stereoscope images showing segments of fractured surfaces characteristics during FCG of (a) T3 material (b) A300 material

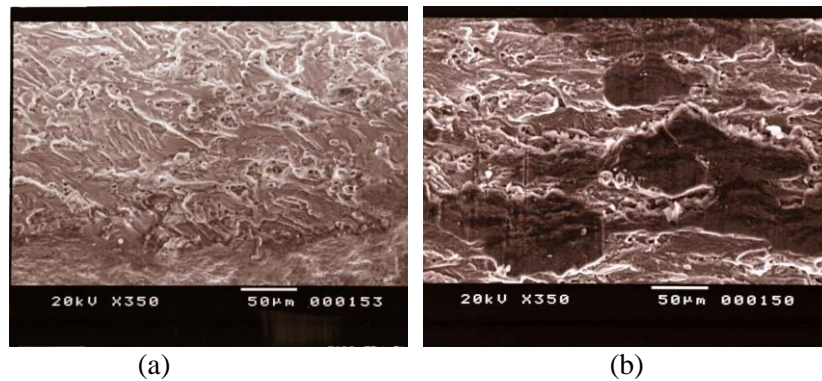


Figure 7. SEM micrograph of fracture surface for Aluminum 2024 (a) T3 condition (b) A300 condition

5 Conclusions

The effect of overaging on fatigue crack growth behavior of 2024 T3 aluminum alloy at intermediate ΔK values was investigated experimentally. The experimental findings showed that:

- Fatigue crack growth rates resistance is enhanced in the overaged material compared to T3 alloy and increases further with the magnitude of temperature.
- The strain hardening exponent in tensile test is higher in overaged material compared to T3 condition and increases further with the magnitude of temperature.
- The basic mechanism that contributes to superior fatigue crack growth resistance in overaged material is increased crack closure due to plasticity effects favoured the lower yield strength and modification of strain hardening characteristics.

Acknowledgments

This research has been co-financed by the European Union (European Social Fund - ESF) and Greek national funds through the Operational Program "Education and Lifelong Learning" of the National Strategic Reference Framework (NSRF) - Research Funding Program: Heracleitus II. Investing in knowledge society through the European Social Fund.

References

- [1] J.G. Kaufman (2000). *Introduction to Aluminum Alloys and Tempers*, ASM International, Ohio.
- [2] Kumar R, Garg S (1989). Effect of Yield Stress and Stress Ratio on Fatigue Crack Closure in 6063-T6 Aluminium Alloy, *Int. J. Pres. Ves. & Piping*, 38, 293-307.
- [3] Putatunda S (1988). Influence of material strength level on fatigue crack closure, *Engineering Fracture Mechanics*, 30, 627-639.
- [4] Petrak G (1974). Strength level effects on Fatigue Crack Growth and Retardation, *Engineering Fracture Mechanics*, 6, 725-733.
- [5] Bray G, Glazov M, Rioja R, Li D, Gangloff R (2001). Effect of artificial aging on the fatigue crack propagation resistance of 2000 series aluminum alloys, *International Journal of Fatigue*, 23, 265-276.
- [6] Sarioglu F, Orhaner F (1998). Effect of prolonged heating at 130°C on fatigue crack propagation of 2024 Al alloy in three orientations, *Mat. science & engineering A*, 248, 115-119.
- [7] Sharma V, Sree Kumar K, Nageswara Rao B, Pathak S (2011). Fatigue crack growth of AA2219 under different aging conditions, *Materials Science and Engineering A*, 528, 4040-4049.
- [8] Garret G, Knott J (1975). Crystallographic fatigue crack growth in Aluminium Alloys, *Acta Metall.*, 23, 841-848.
- [9] Mohammed Noor Desmukh, Pandey R, Mukhopadhyay A (2006). Effect of aging treatments on the kinetics of fatigue crack growth in 7010 aluminum alloy, *Materials Science and Engineering A*, 435-436, 318-326.
- [10] Tzamtzis A, Kermanidis A (2012). Experimental investigation of fatigue crack propagation in 2xxx aluminum alloy with local yield strength gradient at the crack path, *4th International Conference on crack paths*, Gaeta, Italy.
- [11] Huda Z, Taid N, Zaharinie T (2009). Characterization of 2024-T3: An aerospace aluminum alloy, *Materials Chemistry and Physics*, 113, 515-517.
- [12] Dowling N (2006). *Mechanical Behavior of Materials: Engineering Methods fir Deformation, Fracture, and Fatigue*, Third Edition, Prentice Hall.
- [13] Suresh S (1998). *Fatigue of Materials*, 2nd edition, Cambridge University Press, London.
- [14] Elber W (1971). The Significance of Fatigue Crack Closure, *ASTM STP*, 486, 230-242.
- [15] Callister W, Rethwisch D (2010), *Materials science and engineering: An introduction*, 8th edition, Versailles.
- [16] Kermanidis A, Pantelakis Sp (2011). Prediction of crack growth following a single overload in aluminum alloy with sheet and plate microstructure, *Engineering Fracture Mechanics*, 78, 2325-2337.
- [17] Venkateswara K, Bucci R, Jata K, Ritchie R (1991). A comparison of fatigue crack propagation behavior in sheet and plate aluminum-lithium alloys, *Materials Science and Engineering A*, 141, 39-48.
- [18] Kermanidis A, Tzamtzis A (2012). Prediction of fatigue crack propagation in aluminum alloy with local yield strength gradient at the crack path, *Proceedings of 14th International Conference on Mesomechanics*, Budapest.